RSC Advances

ROYAL SOCIETY OF CHEMISTRY

www.rsc.org/advances

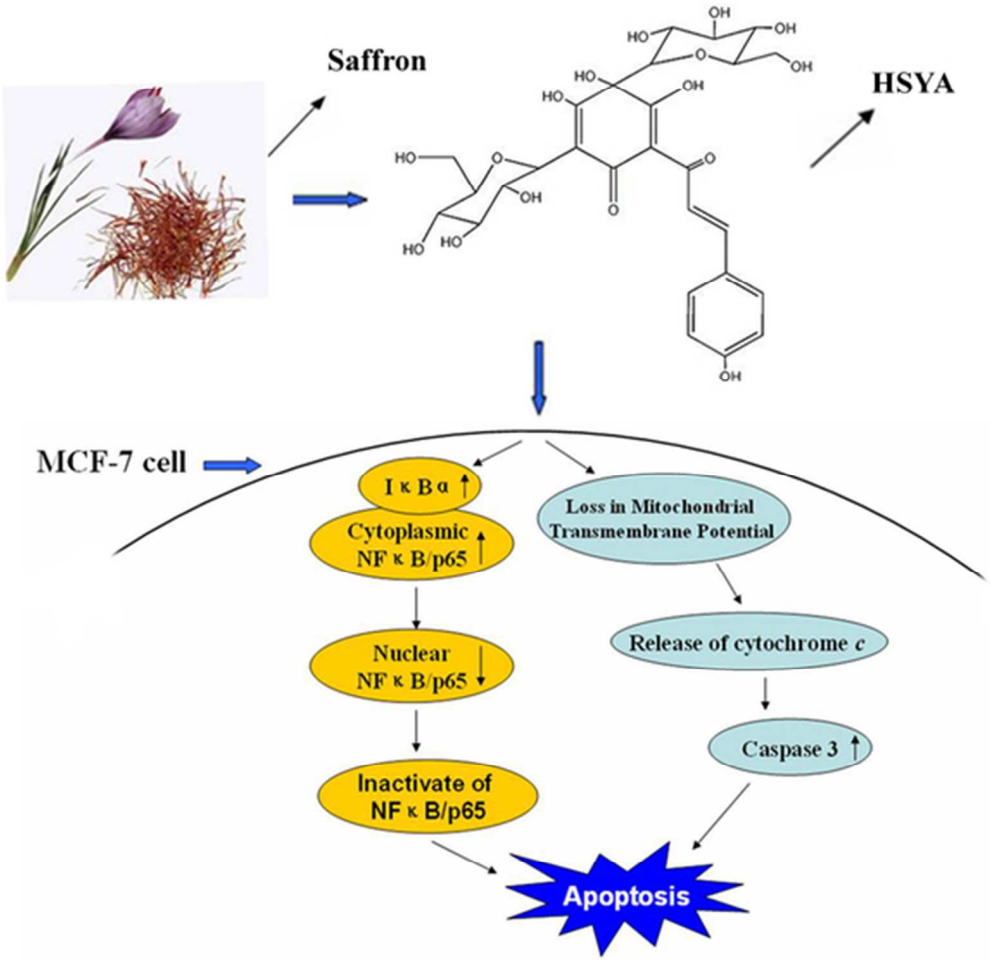

24x23mm (600 x 600 DPI)

Hydroxysafflor yellow A induces apoptosis in MCF-7 cells by blocking NFκB/p65 pathway and loss in mitochondrial transmembrane potential

YuYing Li, Yanzi Wu, Yingying Guan, ZhuanHua Wang*, Liwei Zhang*

Key Laboratory for Chemical Biology and Molecular Engineering of Ministry of Education, Shanxi University, 92 Wucheng Road, Taiyuan, 030006, China

*Corresponding author. Tel.: + 86 351 7019371; Fax: + 86 351 7011499.

E-mail address: zhwang@sxu.edu.cn；lwzhang@sxu.edu.cn

The molecular mechanisms and the possible effects of hydroxysafflor yellow A (HSYA) on the induction of apoptosis in the human breast cancer MCF-7 cells was investigated. The MTT assay showed that HSYA could specifically inhibit the growth of several solid tumor cells in a dose-dependent manner, especially in MCF-7 cells. Analysis by flow cytometry indicated that the apoptosis of MCF-7 cells increased after treatment with HSYA. Moreover, the ROS level increased and cell cycle was blocked when the MCF-7 cells were treated with HSYA. HSYA-induced apoptosis involved Bax and p53 up-regulation, Bcl-2 and CyclinD1 down-regulation, release of cytochrome *c* from the mitochondria to the cytosol, activation of caspase-3, and disruption of the mitochondrial transmembrane potential ($\Delta\psi_m$). In addition, HSYA could inhibit the NFκB/p65 pathway by blocking the NFκB/p65 nuclear translocation. We concluded that HSYA could induce the apoptosis in MCF-7 cells and promote apoptosis through the mitochondrial apoptotic pathway.

Keywords: HSYA， Apoptosis， NFκB/p65， Mitochondrial transmembrane potential

Introduction

Safflower, a widely used traditional Chinese herbal medicine, is the dried flower of *Carthamus tinctorius* L. (Compositae). Safflower consists of mixed chalcone glycosides with the pharmacological activities for the treatment of a variety of cardiovascular and cerebrovascular

diseases. In addition, safflower can treat numerous cycle disorders; it possesses anticancer effects when used alone or in combination with other herbal components.[1, 2]

The extracts from *C. tinctorius* contain several pigments, such as hydroxysafflor yellow A (HSYA), safflower yellow B, safflomin A, safflomin C, and other prevalent pigments.[3,4] Numerous studies have demonstrated that safflower yellow (SY) has various physiological and pharmacological activities, including anti-thrombotic and anti-hypertensive effects. HSYA, which is the main chemical component of the safflower yellow pigments, has been demonstrated to have anti-oxidative activities and myocardial and cerebral protective effects.[5]

HSYA has a chalcone structure and contains a number of phenolic hydroxyl groups. Moreover, its effects may be related to the antioxidant activities of these phenolic hydroxyl groups. HSYA could inhibit the proliferation of human umbilical vein endothelial cells in vitro, as well as the formation of new blood vessels.[4, 6] However, the effective monomeric composition of safflower and its role in the anticancer mechanism is not well known. Therefore, more studies are needed to fully understand the mechanism.

Many physiological processes, such as cell proliferation, cell cycle, and cell apoptosis have significant roles in the occurrence and development of breast cancer cells. Cell apoptosis and cycle arrest are cell-initiated death courses that are controlled by the changes in gene expression and activation. In addition, they are the important mechanisms that maintain the stability of an organism.[7] For cell apoptosis，there are two major signaling pathways: the extrinsic pathway, which acts through ligand-mediated activation of death receptors on the cell surface, and the intrinsic pathway, which acts through the mitochondria. Mitochondria play a critical role in the regulation of various apoptotic processes including drug-induced apoptosis.[8]

The signaling pathways that govern cell proliferation, survival, and oncogenesis are of prime interest in cancer biology. Since the discovery of the mammalian Rel/NF-κB factors, studies have focused on their transcriptional and biological functions, as well as on the mechanisms that control their activities.[9] In normal cells, NF-κB bound to its inhibitor IκB, sequesters the NF-κB·IκB complex in the cytoplasm. Upon stimulation, IκBs are phosphorylated by upstream kinases and degraded through the ubiquitination– proteasome pathway, thus releasing the active NFκB dimer into the nucleus to regulate gene transcription.[10]

Reactive oxygen species (ROS), such as superoxide anion (O^{2-}), hydrogen peroxide (H_2O_2),

and hydroxyl radical (HO•), consist of radical and nonradical oxygen species formed by the partial reduction of oxygen. Cellular ROS are generated endogenously as in the process of mitochondrial oxidative phosphorylation, or they may arise from interactions with exogenous sources such as xenobiotic compounds.[11] ROS can damage DNA, activates apoptosis induced by p53, and plays a key role in the process of the apoptosis occurrence.[12]

In this study, we initially assessed and compared the antitumor effects of HSYA in different human solid tumor cell lines (EC9706, HepG2, HeLa, C6, QBC939, SGC7901, SW480, and MCF-7). Furthermore, we focused on the molecular mechanisms of HSYA on cell cycle and apoptosis against breast cancer MCF-7 cells. Moreover, the ROS level and mitochondrial transmembrane depolarization of MCF-7 cells were assayed after treating the cells with HSYA. The present work will provide important insights on safflower's antitumor mechanism, which can be used as the experimental basis in the full utilization of plant flavonoids.

Materials and methods

Reagents and antibodies

3-(4, 5-Dimethylthiazol-2-yl)-2, 5-diphenyltetrazolium bromide (MTT) was purchased from Sigma (St. Louis, MO, USA). Dulbecco's modified eagle's medium (DMEM, high glucose) was purchased from Hyclone (Logan, UT, USA). Fetal calf serum (FCS) was purchased from the Institute of Hematology (Hang Zhou, China). Annexin V-FITC apoptosis detection kit was purchased from Pharmingen-Becton Dickinson (San Diego, CA, USA). Antibodies against NFκB /p65 and p-IκBα were purchased from Santa Cruz Biotechnology, Inc. (CA, USA). IκBα, COX-IV antibodies were purchased from Biogot Biotechnology, Co., Ltd. (Shanghai, China). Bcl-2, Bax, Caspase-3, p53, p21, Cyclin D1 antibodies, and ROS (Reactive Oxygen Species) assay kit, nuclear and cytoplasmic protein extraction kit and JC-1 fluorescent probe were purchased from Beyotime Institute of Biotechnology, Inc. (Nanjing, China). HistoneH3A, GADPH and β-Tublin antibodies were purchased from Sangon Biotech Co., Ltd. (Shanghai, China). Enhanced chemiluminescence (ECL) kit was purchased from Engreen Biosystem Co., Ltd. (Beijing, China). Total RNA isolation kit was from Takara Biotechnology Co., Ltd. (Dalian, China).

Preparation of HSYA

100 g of *C. tinctorius* soaked in 1000 mL of distilled water after 30 min and 60 °C water bath extraction for 45 min. The extracts were filtered and concentrated under reduced pressure, and the residue was suspended in 300 mL water and separated by polyacrylamide column. The column was washed with the water, 30 % ethanol, and 50 % ethanol, respectively. The elution was purified by MDS column, the column was washed with the water, 5 % ethanol, and 10 % ethanol gradient elution. The eluate fractions were filtered and concentrated under reduced pressure, freeze-drying. Next, the purity of HSYA was confirmed by HPLC at 95 %. The structure of HSYA was identified by nuclear magnetic spectra. The structure of HSYA (3,3',4',5,7- pentahydroxylflavone),[14,15] which has a molecular formula of $C_{27}H_{32}O_{16}$ and relative molecular mass of 612 Da are shown in **Fig. 1**. HSYA was dissolved in sterile dimethyl sulfoxide (DMSO) and stored at −20 °C. The final DMSO vehicle concentration did not exceed 0.1 % (v/v) both in the control and in the treated samples in all experiments. HSYA in DMSO was diluted to various concentrations with the culture medium before each experiment.

Cell lines and culture

Human esophagus cancer cell line EC9706 (was kindly presented by Prof. Ming-rong Wang of Institute of Tumor, Chinese Academy Medical of Sciences, Beijing, China), Human cervical carcinoma cell line HeLa, The human breast cancer cell line MCF-7, human cholangiocarcinoma cell line QBC939, the human hepatoma cell line HepG2, human glioma cell line C6, human gastric carcinoma cell line SGC-7901, and human colorectal cancer cell line SW480 were purchased from the Cell Bank of the Chinese Academy of Sciences (Shanghai, China). EC9706, HeLa, and SW480 cells were cultured in RPMI 1640 medium containing 10 % (v/v) heat-inactivated FCS with 8 U mL^{-1} gentamicin sulfate and 15 mM 4-(2-hydroxyethyl)-1-piperazineethanesulfonic acid (HEPES) under humidified 5% CO_2 atmosphere. MCF-7, QBC939, C6, SGC-7901, and HepG2 cells were cultured in DMEM with 10% fetal bovine serum (FBS), 100 U mL^{-1} penicillin, and 100 U mL^{-1} streptomycin and then incubated at 37 °C with 5 % CO_2.

Cell growth inhibition assays

The cells were plated in 96-well microtiter plates at a density of 1×10^5 cells mL^{-1} in a volume of

100 μL and were permitted to adhere for 24 h before treatment. Various concentrations (50, 100, and 200 μg mL^{-1}) of HSYA were added to the wells, and the plates were incubated for the indicated times. After cells were incubated with 20 μL MTT (5 mg mL^{-1}) for 4 h at 37 °C. After removing the medium and MTT, 150 μL of DMSO was added into each well, and then placed on a plate shaker for 5 min at room temperature. The absorbance at 570 nm for each well was measured using a microtiter plate ELISA reader (Bio-Rad model 550). The mean values for three parallel experiments were calculated. Percentage of inhibition = 1 − (mean experimental absorbance/mean control absorbance) × 100 %.

Staining of apoptotic cells with DAPI

MCF-7 cells from exponentially growing cultures were seeded in six-well plates and allowed to attach for 24 h before treatment. The cells were treated with 100 μg mL^{-1} HSYA for 24 h. After treatment, cells were washed with phosphate-buffered saline (PBS), and re-suspended in a fixation solution (4 % paraformaldehyde) at 4 °C for 10 min. The cells were stained with 4′, 6-diamidino-2-phenylindole (DAPI) (2 mg mL^{-1}) for 5 min at room temperature, and the apoptotic cells were evaluated under a laser confocal microscope (FV1000; Olympus, Tokyo, Japan). The apoptotic cells were identified through nuclear condensation and fragmentation.

Flow cytometric analysis

MCF-7 cells (1×10^5 mL^{-1}) were seeded in a six-well plate containing complete medium and allowed to attach for 24 h. The cells were treated with 25, 50, or 100 μg mL^{-1} HSYA for 24 h and then washed twice with cold PBS. Afterward, the cells were centrifuged at 1,500 ×g for 10 min to collect the cells. The cell apoptosis, cell cycle, and ROS level were analyzed by flow cytometry (FACSCalibur, B-D, USA), respectively. Data analysis was performed using the Cell Quest program.

Apoptosis analysis: Flow cytometric analyses of annexin V-FITC and PI-stained cells were performed using an apoptosis detection kit according to the manufacturer's protocol. The cells were re-suspended in 500 μL of binding buffer, containing 5 μL of fluorescence-conjugated annexin V-FITC, and 1 μL of PI. The suspension was then incubated at room temperature for 30 min in the dark. Afterward, the cells were analyzed using flow cytometry.

Cell cycle analysis: The cells were fixed in 70 % cold ethanol, washed with PBS, and then stained with 100 μL PI (1 mM) and 50 μL RNase A (1 mM) in PBS at room temperature for 30 min in the dark. The cell distribution at the different phases of the cell cycle was analyzed through flow cytometry.

ROS level analysis: The cells were incubated with 1 mL of DCFH-DA (10 μM) at 37 °C for 20 min in the dark. Then, the cells were washed twice and kept in 300 μL of PBS. ROS generation was assessed through flow cytometry.

Measurement of mitochondrial transmembrane potential (MMP, Δψm)

JC-1 is a fluorescent carbocyanine dye, which accumulates in the mitochondrial membrane in two forms (monomers or dimers), depending on mitochondrial membrane potential. Cells with normal polarized mitochondrial membranes emit green-orange fluorescence, and the percentage of cells that emit only green fluorescence is attributable to depolarized mitochondrial membranes. For analyses of mitochondrial membrane potential, ψm, the cells were collected by centrifugation at 1000 × g for 5 min. Briefly, 2×10^5 cells were washed twice with cold PBS and incubated in 500 μL JC-1(10 μg mL^{-1}) for 30 min at 37 °C. After 30 min of incubation in the dark at 37 °C, the cells were analyzed using the flow cytometer (FACSCalibur, B-D, USA). Data analysis was performed using the Cell Quest program.

Preparation for cytosolic and mitochondrial fractions

The cells were prepared for staining according to the cytochrome c-releasing apoptosis assay kit purchased from BioVision (Mountain View, CA, USA). Briefly, 1×10^6 cells were pelleted and washed once with ice-cold PBS. The cells were re-suspended in Cytosol extraction buffer mix containing DTT and protease inhibitors and incubated on ice for 10 min. The lysate was then centrifugated at 1000 × g at 4 °C for 10 min. The supernatants were centrifuged again at 10,000 × g at 4 °C for 30 min. Afterward, the supernatants were collected as cytosolic fractions, and the pellets were resuspended in a mitochondrial extraction buffer mix containing DTT and protease inhibitors for 10 s and used as mitochondrial fractions.

Western blot analysis

To prepare the whole-cell extract, cells were washed twice with cold PBS and lysed in cold

radioimmunoprecipitation assay extraction buffer (1 × PBS, 0.5 % deoxycholic acid sodium salt, 1% Triton X-100, 0.1 % SDS, 1 mM PMSF, 1 % leupeptin, and 1 % aprotinin) for 30 min on ice. The lysates were centrifuged at 12,000×g for 10 min at 4°C, and then the supernatant was collected. To separate cytoplasmic and nuclear fractions of proteins, a nuclear and cytoplasmic protein extraction kit was immediately used for extraction after cell collection. Briefly, cells were mixed with cytoplasmic protein extraction buffer, vortexed at maximum speed, and then incubated for 15 min on ice. After centrifugation at 12,000 ×g for 5 min at 4 °C, the suspension, including the cytoplasmic protein, was collected. Nuclear protein extraction buffer was added into the pellet, and then the resulting mixture was vigorously shaken. After incubation for 30 min on ice, the suspension was centrifuged at 12,000×g at 4 °C for 5 min. The resulting supernatant was the nuclear fraction. Protein concentrations were measured using the BCA protein assay kit (Beyotime Institute of Biotechnology). Total protein samples were transferred onto PVDF membrane after electrophoretic separation in 10 % SDS polyacrylamide gel. After blocking with 5 % non-fat milk in tris-buffered saline containing Tween-20 (0.1 %) (TBST) for 2 h at room temperature, the membranes were incubated at 4 °C overnight with the primary antibody and then washed five times with TBST (0.05 %). Afterward, the membranes were incubated with horseradish peroxidase-conjugated secondary antibodies at room temperature for 2 h. The membranes were washed thrice in TBST, incubated with an enhanced chemiluminescence western detection system (Engreen), and exposed to an X-ray film.

RNA isolation and qRT-PCR

Total RNA was isolated from cells using RNAiso Plus according to the manufacturer's instructions. Afterward, RNA was reverse transcribed to cDNA using the Primescripted RT reagent kit with gDNA eraser (Takara Biotechnology, Dalian, China). qRT-PCR amplification and detection were performed using the SYBR Premix Ex Taq^{TM} (QIAGEN, China) according to the manufacturer's protocol. PCR reaction was performed on RT-PCR Machine 7500 Fast (Applied Biosystems) at 95 °C for 5 min for denaturation, followed by 40 cycles at 95 °C for 10 s and 60 °C for 1 h. The reaction products were analyzed using software provided by the onboard software from the RT-PCR machine. We used GADPH as the reference gene, and the relative expression levels were analyzed using the $2^{(-\Delta\Delta CT)}$ method. Table 1 lists the primer sequences used. The

primers in our experiments were synthesized by Invitrogen Biotechnology Co., Ltd. (Shanghai, China).

Statistical analysis of data

The data were presented as mean ± SEM. Statistical analysis was performed using ANOVA followed by Dunnett *t*-test, $P < 0.05$ was considered statistically significant. All the figures shown in this paper were obtained from at least three independent experiments.

Results

HSYA inhibited the proliferation of tumor cells

In this study, MTT assay was used to detect the proliferation inhibition of HSYA on several tumor cells in vitro. The result showed (Fig. 2) that HSYA could significantly inhibit the proliferation of several tumor cells in a dose-dependent manner. Within concentrations of 50 to 200 μg mL^{-1}, HSYA significantly inhibited the proliferation of MCF-7, SGC-7901, SW480, and HeLa cells. Moreover, the inhibition increased with increasing drug concentration. When the cells were treated with 200 μg mL^{-1} HSYA for 24 h, the proliferation inhibition rate of the MCF-7, SGC-7901, SW480, and HeLa cells were 57.6 %, 51.7 %, 53.5 % and 50.2 %, respectively. Meanwhile, HSYA was found little effect on normal cells HL7702 and almost no effect on human normal colorectal cells FHC (data not shown). Thus, the growth inhibition effects of HSYA on MCF-7 cells were most significant at the same concentrations, and the data for each group show considerable differences compared with that of the control group.

HSYA induced apoptosis in MCF-7 cells

To determine whether the HSYA-mediated growth inhibition of MCF-7 cell lines is associated with apoptosis, we used DAPI to investigate the changes in the cells' nuclei. As clearly shown in Fig. 3A the stained nuclei in the control group were uniform and had low-intensity uniform fluorescence. By contrast, when cells were treated with 100 μg mL^{-1} HSYA, the apoptotic cells showed irregularly stained nuclei because of chromatin condensation and nuclear fragmentation, as well as irregular shapes and small amounts of apoptotic bodies.

Simultaneous staining with annexin V-FITC and PI distinguished between healthy, early

apoptotic, late apoptotic and dead cells. After 24 h of treatment with or without different concentrations of HSYA, apoptosis in human MCF-7 cells was analyzed by flow cytometry. Fig. 3B showed that the percentages of apoptotic cells (including early- and late-apoptotic cells) were 5.0 % (3.3 % and 1.7 %) when the cells were not treated with HSYA (control group), but were 32.1 % (15.1 % and 17.0 %) and 68.2 % (46.7 % and 21.5 %) when cells were treated with 50 or 100 μg mL^{-1} HSYA, respectively. The apoptosis rate was significantly higher than that of the control group. These results suggest that HSYA significantly induces apoptosis in MCF-7 cells.

HSYA could inhibit cell growth by blocking the cell cycle

As cell proliferation is regulated by the cell cycle, the Sub-G1 phase of the cell cycle can also be used to determine the apoptosis. Flow cytometry was used to analyze HSYA effect on MCF-7 cell cycle distribution. Fig. 4 showed that the cell count in Sub-*G1* phase was 3.57 % when the cells were not treated with HSYA (control group), but were 6.17 % and 13.77 % when the MCF-7 cells were treated with 50 or 100 μg mL^{-1} HSYA for 24 h, respectively. These data provide evidence for apoptosis. Meanwhile, the cell counts in *G0/G1* and *G2/M* phase were 80.47 % and 2.08 %, respectively, when the cells were not treated with HSYA (control group). However, the cell counts were 80.46 % and 67.61 % in the *G0/G1* phase, and were 7.04 % and 17.37 % in the *G2/M* phase when MCF-7 cells were treated with 50 or 100 μg mL^{-1} HSYA for 24 h, respectively. The cell count significantly increased in the *G2/M* phase, but the cell count decreased in the *G0/G1* phase. These results indicate that HSYA could inhibit cell growth by blocking the cell cycle at the *G2/M* phase.

HSYA induced ROS generation in MCF-7 cells

DCFH-DA can be deacetylated by intracellular esterase to nonfluorescent DCFH, which can be oxidized by ROS, resulting in the formation of fluorescent compound DCF. The fluorescence intensity of DCF is proportional to the amount of ROS produced by the cells.

The data in Fig. 5 indicated that the fluorescence intensity was 279.78 in the control group. The values were 619.80 and 639.01 when the MCF-7 cells were treated with 50 or 100 μg mL^{-1} HSYA for 24 h, respectively. Therefore, HSYA could significantly enhance the ROS level in MCF-7 cells. The ROS trigger can change the balance of cell oxidation–reduction, which is the

key target of intracellular oxidative stress that promotes cell apoptosis. [15]

Mitochondrial membrane depolarization and cytochrome c release during HSYA-induced apoptosis

Mitochondrial transmembrane potential (MMP, $\Delta\psi$m) and mitochondrial permeability changes during apoptosis play an important role in the process.[16] Cytochrome c release from mitochondria is a critical step in the apoptotic cascade as this activates downstream caspases. Cytochrome c is located in the space between the inner and outer mitochondrial membranes. An apoptotic stimulus, such as a change in MMP, triggers the release of cytochrome c from the mitochondria into the cytosol.[7] Mitochondrial membrane depolarization and cytochrome c release have both been proposed as early irreversible events in the initiation of the cell death program. Permeability transition pore (PTP), a complex composed of several polypeptides at the membrane of mitochondria, changes a dissipation of the inner mitochondrial transmembrane potential and an increase in the matrix volume that induces the mechanical disruption of the outer mitochondrial membrane, leading to cytochrome c release.[17]

To determine the involvement of the mitochondrial mediated pathway in the HSYA -induced apoptosis of tumor cells, we investigated the changes in MMP ($\Delta\psi$m) using the JC-1 fluorescent probe. After HSYA treatment of MCF-7 cells, the mitochondrial membrane potential dye, which was analyzed via flow cytometry, showed that R2:R1 was 37.95 % in the control group, whereas R2:R1 was 57.54 % and 74.87 % when MCF-7 cells were treated with 50 or 100 μg mL^{-1} HSYA. The data resulted in a rapid dissipation of $\Delta\psi$m in a dose-dependent manner (Fig. 6A). A collapse of the $\Delta\psi$ m was detected as indicated by loss of red fluorescence as early as 24 h after 50 or 100 μg mL^{-1} of HSYA treatment. This change reached its maximum after treatment with 100 μg mL^{-1} HSYA treatment.

To examine cytochrome c release in HSYA-treated MCF-7 cells, we conducted Western blot assay of the cytosolic and mitochondrial fractions. The mitochondria and cytoplasm of cells were extracted and analyzed through SDS-PAGE electrophoresis and Western blot assay. As shown in Fig. 6B, the increased in cytochrome c levels occurred in the cytosolic fraction and was observed 24 h after 50 or 100 μg mL^{-1} HSYA treatment, but more sigficantly when treated with 100 μg mL^{-1} HSYA. Meanwhile, along with a concurrent decrease in mitochondrial cytochrome c, suggesting

the involvement of mitochondria in HSYA -induced apoptosis.

HSYA regulated apoptosis and cycle factor expression

Cell apoptosis is regulated by the expression of several genes, and one of the most typical is the Bcl-2 family. The mitochondria-mediated intrinsic apoptotic pathway is also controlled by the members of the Bcl-2 family. The Bcl-2 family can be divided into two categories: pro-apoptosis and anti-apoptotic genes. Bcl-2 is an anti-apoptotic gene that can regulate the apoptosis pathway and cell death.[18, 19] In this study, MCF-7 cells were treated with 50 or 100 μg mL^{-1} HSYA, and the total RNA was extracted. Oligo (dT) was used as a primer for the reverse transcription, and the newly synthesized cDNA was amplified through qRT-PCR. The result in Fig. 7A showed that the level of pro-apoptotic gene *Bax* significantly improved, whereas the anti-apoptotic gene *Bcl-2* levels decreased when MCF-7 cells were treated with 50 or 100 μg mL^{-1} HSYA. These results suggested that HSYA-induced MCF-7 cell apoptosis might be involved in the regulation of the Bcl-2 family.

The accumulation of p53 triggered apoptosis and led to the release of cytochrome c from mitochondria to cytosol. Caspase-3 played key roles in the post-mitochondrial apoptotic pathway including the activation of several caspases which are the hallmarks of apoptosis.[20, 21] The tumor characteristics include uncontrolled cell growth and abnormal cell proliferation, differentiation, and apoptosis. Moreover, cell cycle disorder is the main mechanism involved.[22] Cyclin D1 could induce cell growth by promoting the cell cycle, and is known as an oncogene. Cyclin D1 overexpression is an important factor in the malignant transformation of tumor cells. Combined with an inactivated p53, cyclin D1 overexpression may lead to uncontrolled cell proliferation and even occurrence of tumor.

The qRT-PCR result (Fig. 7A) demonstrated that in the apoptosis MCF-7 cells treated with 50 or 100 μg mL^{-1} HSYA, the expression of cycle regulators *p53 and p21* increased, and the level of *Cyclin D1* decreased. These results suggest that HSYA may induce MCF-7 cell apoptosis by inhibiting MCF-7 cell growth through the down-regulation of *bcl-2* and *cyclin D1*, up-regulate the expression of *p53 and p21*, and lead to the over-expression of *Bax*.

The Western blot result in Fig. 7B showed that, the expression of pro-apoptosis protein Bax in the apoptosis cells induced by HSYA significantly increased, whereas the expression of

antiapoptotic Bcl-2 proteins decreased and that of caspase-3 increased. These results indicated that the regulation of the Bcl-2 family may be involved in the apoptosis induced by HSYA. The increased caspase-3 activity coupled with apoptosis induction indicates that HSYA probably induced apoptosis through the caspase-3 signaling pathway in the MCF-7 cells. In addition, in Fig. 7C showed that, the expression level of p53 and that of the cell cycle regulation factors significantly increased, whereas the CyclinD1 protein expression decreased. These results were consistent with the results of qRT-PCR. Therefore, HSYA inhibited the proliferation of breast cancer cells and induced apoptosis; it was also closely linked with cell cycle arrest.

HSYA inhibited the activation of NF-κB/p65 signaling pathway in MCF-7 cells

The eukaryotic transcription factor NFκB exists in a variety of cells, and is involved in the transcriptional regulation of numerous genes that express cytokines, cytokine receptors, and cell adhesion, as well as inflammatory and immune response factor-mediated apoptosis, cell cycle, cell differentiation, cell migration, as well as cell resistance to chemotherapy and proteins of other regulatory processes. NF-κB activation can regulate the expression of anti-apoptotic and pro-apoptotic proteins, as well as the expression of the cell cycle proteins, including p53 and cyclin D1.[23, 24] IκBα has the most crucial role as the molecular switch in the activation of the NF-κB pathway, in which the phosphorylation of IκBα is a key.[25]

When MCF-7 cells were treated with 50 or 100 μg mL^{-1} HSYA for 24 h, the cytosolic fractions and nuclear extracts were separated. The Western blot assay results (Fig. 8) showed that the expression of p65 protein significantly increased in the cytoplasm, but decreased in the nucleus. In addition, the expression of phosphorylated IκBα significantly decreased and then increased the expression of IκBα, these results suggested that HSYA may induce apoptosis and block the cell cycle by inhibiting the NF-κB/p65 signaling pathway.

Discussions

Safflower is an important traditional Chinese medicine that affects blood circulation and blood stasis, and relieves pain. Safflower has low toxicity in vivo, and is an abundant natural resource. Safflower has antitumor effects against a variety of cancers, such as liver, cervical, stomach, esophageal, and breast cancers.[26, 27] Safflower yellow pigment is extracted from petals with

natural red pigments, which are composed of a variety of flavonoids, and have substantial pharmacological activity. HSYA (hydroxysafflor yellowA) is considered to be the main and most effective ingredient of safflower yellow pigment, could clear a hydroxyl group, inhibition of lipid peroxidation, protecting cell membranes.[28, 29] However, the effects of HSYA on breast cancer cells and its antitumor mechanism are still not well understood. Moreover, only a limited number of studies on the active ingredients of saffron and their antitumor mechanisms have been conducted. In our previous study, we have separated and obtained hydroxysafflor yellow A. Moreover, we have simultaneously investigated the anticancer activity of the extract using MTT assay and the proliferation of MCF-7 cells treated with HSYA. The results showed that HSYA could significantly inhibit the proliferation of MCF-7 cells in a dose-dependent manner. Moreover, HSYA caused chromatin condensation and nuclear fragmentation. Thus, we had concluded that HSYA induces MCF-7 cell apoptosis.

Apoptosis, one of the most fundamental biological processes in eukaryotes is a well-defined cell-death process. There are two main pathways that lead to apoptosis, ‘‘extrinsic’’ and ‘‘mitochondrial’’ pathway. The mitochondrial apoptotic pathway begins when an injury occurs within the cell. Intrinsic stresses such as oncogenes, hypoxia, survival factor deprivation, and ROS can activate the intrinsic apoptotic pathway.[30]

Numerous studies have confirmed that almost all apoptosis stimulating factors can cause structural damage and mitochondrial dysfunction.[31] Mitochondrial transmembrane potential (MMP, $\Delta\psi$m) and mitochondrial permeability changes during apoptosis play an important role in the process.[16] Apoptosis can occur via the caspase-independent apoptotic pathway. Caspase-3, a key effector caspase, can be activated by several activated initiator caspases such as caspase-9, whose activation is achieved within an apoptosome that consists of a large caspase-activating complex formed by apoptotic protease-activating factor 1, cytochrome c, and dATP. [17]

Cytochrome c release from mitochondria is a critical step in the apoptotic cascade as this activates downstream caspases. Cytochrome c is located in the space between the inner and outer mitochondrial membranes. An apoptotic stimulus, such as a change in MMP, triggers the release of cytochrome c from the mitochondria into the cytosol where it binds to Apaf-1. The cytochrome c/Apaf-1 complex activates caspase-9, which then activates caspase-3 and other downstream caspases.[32, 33] The present study proved that HSYA caused the loss of mitochondrial membrane

potential ($\Delta\psi$m), release of cytochromec from the mitochondrial intermembrane space into the cytosol and proteolytic activation of caspase-3.

The mitochondria-mediated intrinsic apoptotic pathway is also controlled by the members of the Bcl-2 family. Many studies have shown that the ratio between bax/bcl-2 proteins decides the strength of apoptosis inhibition by key factors; therefore, bax is a very important pro-apoptotic gene.[34] This study focused on bcl-2 and bax proteins. The tumor suppressor protein p53 is a key regulator of multiple cellular processes, and evidence suggests that apoptosis is critical for its tumor suppressor function. P53 can increase the expression of Bax levels, and reduce the Bcl-2 expression to promote cell apoptosis.[35]

The susceptibility of proliferating cells to certain apoptosis inducement often depends on the cell cycle. The damage level of physical and chemical stimuli to the cells depends on the balanced regulation of each cell cycle regulatory factor.[36] CyclinD1 is a promoter of the cell cycle, and can be used with a variety of oncogenes to promote mutual transformation between the cells. CyclinD1 can inhibit p21 activity, resulting in cell cycle arrest and blocking cell proliferation.[37] The results of our study indicate that HSYA could down-regulate the expressions of CyclinD1 and Bcl-2 and promote the up-regulation of Bax and p53, thereby blocking the cell cycle in the G2/M phase to induce apoptosis of MCF-7 cells.

In addition, we studied the reactive oxygen species (ROS) when MCF-7 cells were treated with 50 or 100 μg mL^{-1} HSYA. ROS is produced by oxidative stress and DNA damage, plays a key role in the process of the apoptosis occurrence. The antiapoptotic proteins Bcl-2 can regulate and maintain intracellular antioxidant activities, and is mainly found in regions where ROS is produced. These regions include the mitochondrial membrane, endoplasmic reticulum membrane, and nuclear membrane and so on.[38] In response to death stimuli, ROS accumulation and alterations in response to death stimuli are considered early signals of apoptosis.[39] Our study showed that HSYA could induce ROS generation, in a dose dependent manner.

The activity of NF-κB/Rel transcription factors can down-modulate apoptosis in normal and neoplastic cells of the hematologic and of other origins.[40] It was reported that nuclear transcription factor-κB is a very potential targets in the treatment of breast cancer; NFκB is widely involved in the regulation of BC initiation, proliferation, angiogenesis and metastasis. The overexpression of NFκB subunits enhances the expression of NFκB responsive genes that contribute to BC

progression. The use of NFκB inhibitor is a potentially important therapy.[41] In other words, the role of phosphorylation and the interaction between proteins determine the specificity of the NF-κB activity. This study showed that HSYA might inhibit the NFκB/p65 signaling pathways, thereby inducing MCF-7 cell apoptosis.

In summary, the potential anticancer activity of HSYA against human MCF-7 cells was investigated. HSYA exhibited a strong inhibitory effect against the growth of MCF-7 cells in vitro. The anticancer activity of HSYA could be attributed, in part, to its induction of apoptosis in cancer cells by involving Bax and p53 up-regulation, Bcl-2 and Cyclin D1 down-regulation, inducing ROS generation, causing mitochondrial release of cytochrome c into the cytosol, loss in $\Delta\psi m$ and caspase-3 activation. Moreover, HSYA could inactivate the NFκB/p65 pathway in MCF-7 cells by significantly decreasing the expression of phosphorylated IκBα, increasing the expression of IκBα, and blocking NFκB/p65 nuclear translocation. These effects proved the role of HSYA in inducing cell apoptosis. The findings in the present study provided new ideas for the use of safflower and other natural herbs in anti-tumor applications.

Acknowledgements

This work was supported by National Natural Science Foundation of China (No. 31171659) funding, Scientific and Technological Innovation Programs of Higher Education Institutions in Shanxi (2012004), and the Natural Science Foundation of Shanxi Province (No.2011011035-4).

References

1 Y.H. Jin, H. Yim, J.H. Park and S.K. Lee, Biochem. Biophys. Res. Commun.，2003, **305**, 974–980.

2 Z. Lian, K. Niwa, J. Gao, K. Tagami, H. Mori and T. Tamaya, Cancer Detect. Prev.，2003, **27**, 147–154.

3 HO. Pae, H. Oh, Y.G. Yun, G.S. Oh, S.I. Jang, K.M. Hwang, T.O. Kwon, H.S. Lee and H.T.Chung, Pharmacol. Toxicol.，2002, **91**, 40–48.

4 P.H. Nie, L. Zhang, W.H. Zhang, W.F. Rong and J.M. Zhi, J. Ethnopharmacol.，2012, **139**, 746–750.

5 B. Zang, M. Jin,; N. Si, Y. Zhang, W. Wu and Y. Piao, Yao Xue Xue Bao，2002, **37**, 696–699.

6 Y. Tian, Z.F. Yang, Y. Li, Y. Qiao, J. Yang, Y.Y. Jia and A.D. Wen, J. Ethnopharmacol., 2010,**129**, 1–4.

7 Y.Y. Li, Z. Zhang, Z.H. Wang, H.W. Wang, L. Zhang and L. Zhu, Toxicol. Lett., 2009, **189**, 166–175.

8 R. Khosravi-Far and M.D. Esposti, Cancer Biol. Ther., 2004, **3**, 1051–1057.

9 B. Rayet and C. Gélinas, Oncogene, 1999, **18**, 6938–6947.

10 D.K. Biswas and J.D. Iglehart, J. Cell Physiol., 2006, **209**, 645–652.

11 P.D. Ray, B.W. Huang and Y. Tsuji, Cell Signal, 2012, **24**, 981–990.

12 P. Li, Q.L. Zhao, L.H. Wu, P. Jawaid, Y.F. Jiao, M. Kadowaki and T. Kondo, Apoptosis, 2014,**19**, 1043–1053.

13 M.L. Guo, G. Zhang, W. Zhang, H.M. Zhang and Z.W. Su, Zhongguo Zhong Yao Za Zhi, 2006, **31**, 1234–1236.

14 Y. K. Wang, P. Zhi and L. W. Zhang, Food Science, 2013, **34**, 29–32. (Article in Chinese)

15 J. Fang, H. Nakamura and A.K. Iyer, J. Drug Target, 2007, **15**, 475–486.

16 D.D. Newmeyer and S. Ferguson-Miller, Cell, 2003, **112**, 481–490.

17 R. Roggero, V. Robert-Hebmann, S. Harrington, J. Roland, L. Vergne, S. Jaleco, C. Devaux and M. Biard-Piechaczyk, J. Virol., 2001, **75**, 7637–7650.

18 M.J. Kim, Y.J. Kim, H.J. Park, J.H. Chung, K.H. Leem and H.K. Kim, Food Chem. Toxicol.,2006, **44**, 898–902.

19 H.J. Woo, S.J. Lee, B.T. Choi, Y.M. Park and Y.H. Choi, Exp. Mol. Pathol., 2007, **82**, 77– 84.

20 K. M. Boatright and G. S. Salvesen, Current Opinion in Cell Biology, 2003, **15**, 725–731.

21 R. Zhao, X. Gao, Y. Cai, X. Shao, G. Jia, Y. Huang, X. Qin, J. Wang and X. Zheng, Carbohydrate Polymers, 2013, **96**, 376–383.

22 A. Echalier, J.A. Endicott and M.E. Noble, Biochim. Biophys. Acta., 2010, 1804, 511– 519.

23 M.S. Hayden and S. Ghosh, Cell, 2008, **132**, 344–362.

24 H. Fukushima, A. Matsumoto, H. Inuzuka, B. Zhai, A.W. Lau, L. Wan, D. Gao, S. Shaik, M. Y uan, SP. Gygi, E. Jimi, J.M. Asara, K. Nakayama, K.I. Nakayama and W. Wei, Cell Rep., 2012, **1**, 434 – 443.

25 E. Mathes, E.L. O'Dea, A. Hoffmann and G. Ghosh, EMBO. J., 2008, **27**, 1357–1367.

26 W.T. Loo, M.N. Cheung and L.W. Chow，Life Sciences，2004, **76**,191 – 200.

27 S.Y. Xi, Q. Zhang, C.Y. Liu, H.M. Sun, G.L. Ge, W. Cui, H. Xie, L.T. Liu and X.M.GAO, Beijing zhong yi yao da xue xue bao, 2009, **5**,331–335. (article in Chinese)

28 S.Y. Ye and W.Y. Gao, Arch. Pharm. Res., 2008, **31**, 1010–1015.

29 Q. Yang, Z.F. Yang, S.B. Liu, X.N. Zhang, Y. Hou, X.Q. Li, Y.M. Wu, A.D. Wen and M.G. Zhao, Neurochem. Res., 2010, **35**, 1353–1360.

30 W. Jiang, L. Chen, X.J. Zhang, J. Chen, X.C. Li, W.S. Hou and N. Xiao, Neuroscience, 2014, **68**, 66 –74.

31 P. Marchetti, M. Castedo, S.A. Susin, N. Zamzami, T. Hirsch, A. Macho, A. Haeffner, F.Hirsch, M. Geuskens and G. Kroemer, J. Exp. Med., 1996, **184**, 1155–1160.

32 P. Li, D. Nijhawan, I. Budihardjo, S.M. Srinivasula, M. Ahmad, E.S. Alnemri and X. Wang, Cell, 1997, **91**, 479–489.

33 X. Liu, C.N. Kim, J. Yang, R. Jemmerson and X. Wang, Cell, 1996, **86**, 147–157.

34 X. Lei, Y. Chen, G. Du, W. Yu, X. Wang, H. Qu, B. Xia, H. He, J. Mao, W. Zong, X. Liao, M. Mehrpour, X. Hao and Q. Chen, FASEB. J., 2006, **20**, 2147–2149.

35 W.T. Lee and C.W. Chang, Mol. Cell Biochem., 2010, **343**, 271–279.

36 A.B. Coffin, E.W. Rubel and D.W. Raible, J. Assoc. Res. Otolaryngol., 2013, **14**, 645–659.

37 I. Ayed-Boussema, C. Bouaziz, K. Rjiba, K. Valenti, F. Laporte, H. Bacha and W. Hassen, Toxicology in Vitro., 2008, **22**, 1671–1680.

38 D. Morales-Cano, E. Calviño, V. Rubio, A. Herráez, P. Sancho, M.C. Tejedor and J.C.Diez, Exp. Toxicol. Pathol., 2013, **65**, 1101–1108.

39 S. Desagher and J.C. Martinou, Trends. Cell. Biol., 2000, **10**, 369–377.

40 D. Cilloni, F. Messa, F. Arruga, I. Defilippi, A. Morotti, E. Messa, S. Carturan, E. Giugliano, M. Pautasso, E. Bracco, V. Rosso, A. Sen, G. Martinelli, M. Baccarani and G. Saglio, Leukemia, 2006, **20**, 61–67.

41 J. Ling and R. Kumar, Cancer Lett., 2012, **322**, 119–126.

Figure legends

Figure. 1. The chemical structure of hydroxysafflor yellow A HSYA, the molecular formula was determined to be $C_{27}H_{32}O_{16}$, the relative molecular masses is 612 Da.

Figure. 2. Inhibition of HSYA on the proliferation of in the human solid tumor cells Different cells were incubated with various concentration of HSYA for 24 h, respectively. The color intensity was measured using a microtiter plate reader (Bio-Rad model 550) at 570 nm. The data were represented as mean values ± standard of three independent experiments. *p<0.05, **P<0.01 *vs* control.

Figure. 3. Effect of HSYA on MCF-7 cell apoptosis (A) Control (0.1% DMSO, 24 h); 100 μg mL^{-1}) HSYA treated MCF-7 cells for 24 h. MCF-7 cells were fixed with 4% paraformaldehyde and stained with DAPI (2 μg mL^{-1}) for 15 min, detected the morphological features of nucleus by fluorescence microscopy(400×). (B) Control group (0.1% DMSO, 24 h); MCF-7 cells were treated with 50 or 100 μg mL^{-1} HSYA for 24 h, respectively, collected and washed with cold PBS (pH 7.6), re-suspended in 500 μL of binding buffer, containing 5 μL of fluorescence-conjugated annexin V-FITC and 1 μL of PI, then incubated for 30 min in the dark at room temperature. Following this, the cells were analyzed by flow cytometry.

Figure. 4. Effect on cell cycle distribution of MCF-7 cells of HSYA by flow cytometric analysis

(A, B) Control group (0.1 % DMSO, 24 h); MCF-7 cells were treated with 50 or 100 μg mL^{-1} HSYA for 24 h, respectively, collected and washed with cold PBS (pH7.6), suspended in 100 μL of binding buffer, stained with PI (10 mg mL^{-1}), incubated for 30 min at 4 °C. The cell cycle was analyzed using flow cytometry. (C, D) The result showed the cell cycle distribution of every independent experiment by flow cytometry.

Figure. 5. Flow cytometric analysis of intracellular ROS. Control group (0.1 % DMSO, 24 h); Cells were incubated with 50 or 100 μg mL^{-1} HSYA for 24 h. The cells were incubated with 100 μM DCFH-DA for 20 min at 37 °C and washed with serum-free medium to remove extracellular DCFH-DA. Then the ROS level was analyzed by flow cytometry, the result showed the relative ROS level of every independent experiment by flow cytometry.

Figure. 6. The Effect of rBTI on the changes in mitochondrial membrane potential (A) Control group (0.1 % DMSO, 24 h); Cells were incubated with 50 or 100 μg mL^{-1} HSYA for 24 h. Mitocapture was added to the cells, and incubated at 37 ˚C in CO_2 incubator for 15-20 min. Cells were analyzed immediately by flow cytometry. (B) MCF-7 cells were exposed to 50 or 100 μg mL^{-1} HSYA for 24 h, after which cytosolic and mitochondrial fractions were prepared. The levels of cytochrome c in these fractions were examined by Western blot. In a parallel gel of cytosolic fraction, GADPH and COX-IV were used as loading controls. The experiments were repeated three times with similar results. (C) The amount of every protein was quantified by the integrated density (Image J) of each band.

Figure. 7. Expression of the regulation factor in MCF-7 cells (A) MCF-7 cells were treated with HSYA at the concentration of 50 or 100 μg mL^{-1} for 24 h. The qRT-PCR was carried out for each condition with 3 biological repeats and 3 experimental repeats; the average fold changes on mRNA level of cell apoptosis and cycle genes are shown. The graph displayed the mean of three independent experiments, *, $p < 0.05$, **, $p < 0.01$ statistically significant. (B, C) MCF-7 cells were treated as (A). Cells were lysed and equal amounts of proteins were separated by SDS-PAGE, transferred to PVDF membrane, and immunoblotted with antibodies against Bax, Bcl-2, Caspase-3, p53, Cyclin D1, respectively. β -Tublin was used as a loading control. And the amount of every protein was quantified by the integrated density (Image J) of each band.

Figure. 8. Expression level of NF-κB regulation factors were detected by western blot analysis (A, C) MCF-7 cells were treated with HSYA at the concentration of 50 or 100 μg mL^{-1} for 24 h. Cytoplasmic and nuclear extracts representing equal numbers of cells were analyzed by Western blotting using the indicated antibodies. After transferring onto the membrane the blots were probed with antibodies against p65, IκBα, p-IκBα. HistoneH3A and β-Tublin were used as loading controls. (B, D) The amount of every protein was quantified by the integrated density (Image J) of each band.

Figure 1

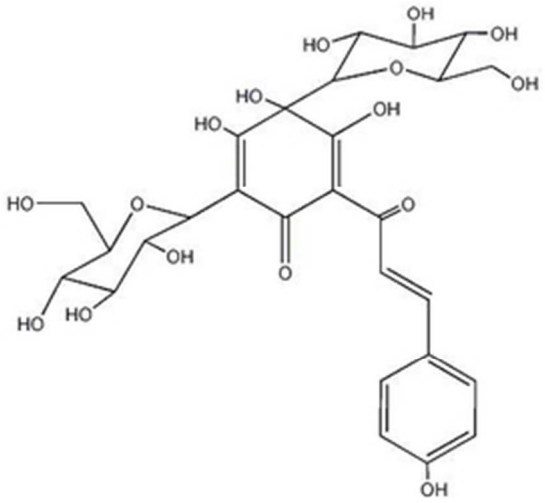

12x14mm (600 x 600 DPI)

Figure 2

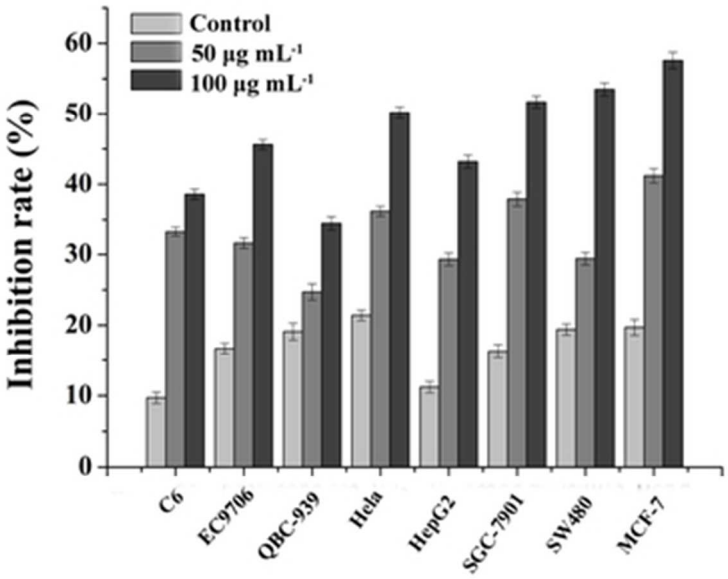

16x15mm (600 x 600 DPI)

Figure 3

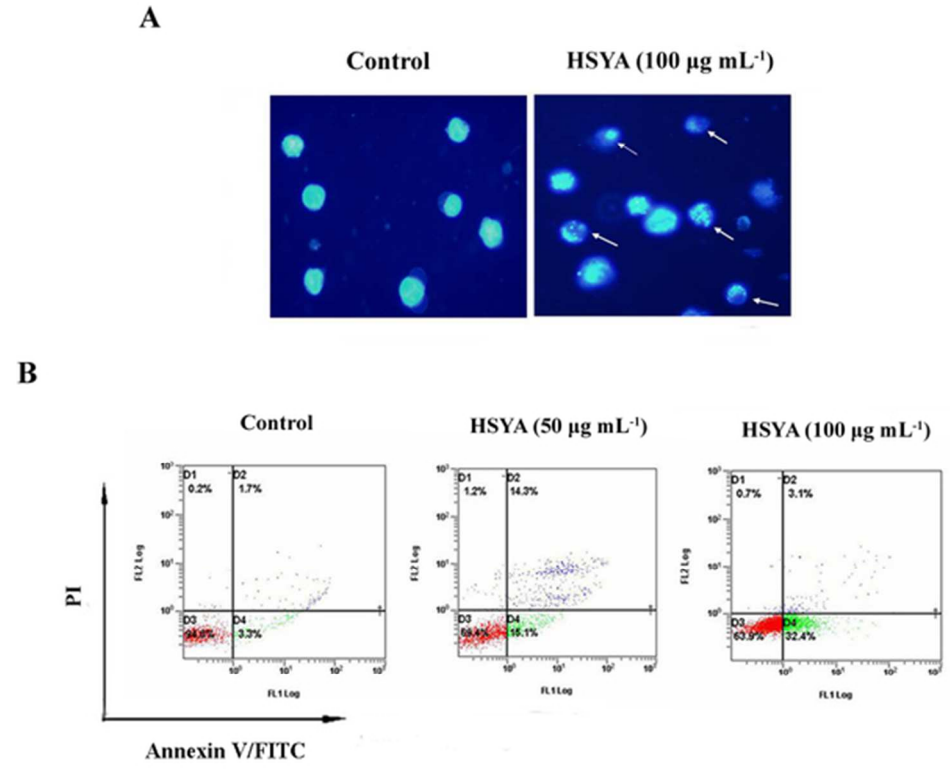

27x22mm (600 x 600 DPI)

Figure 4

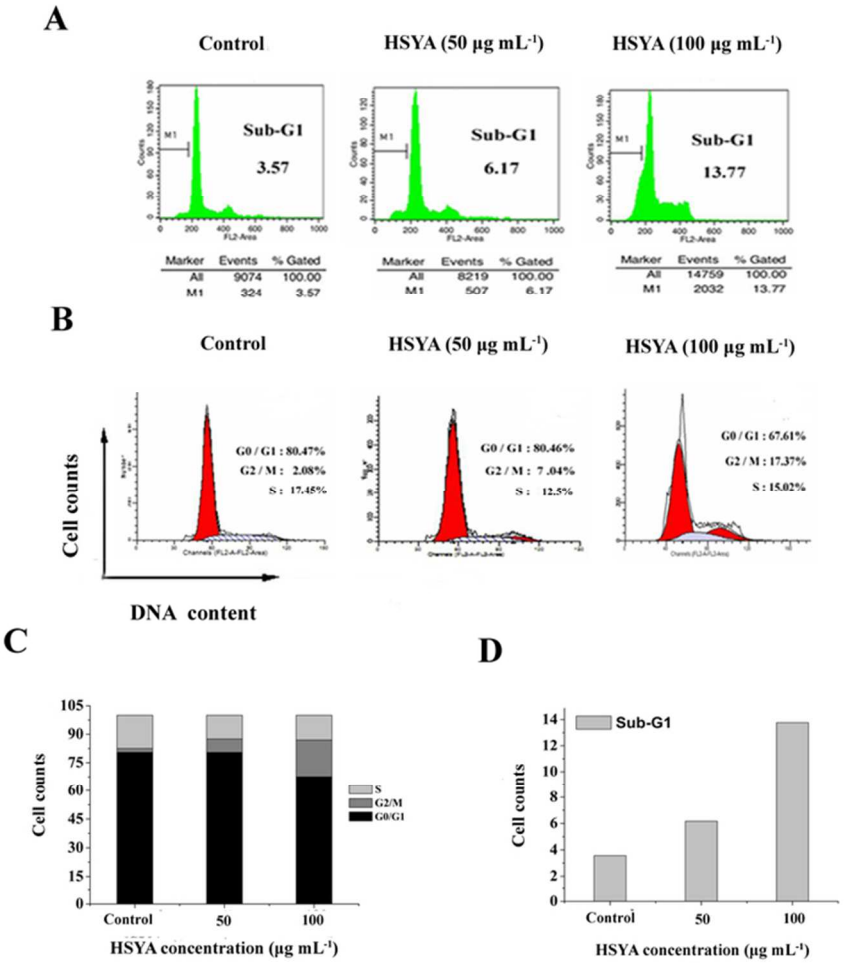

34x37mm (600 x 600 DPI)

Figure 5

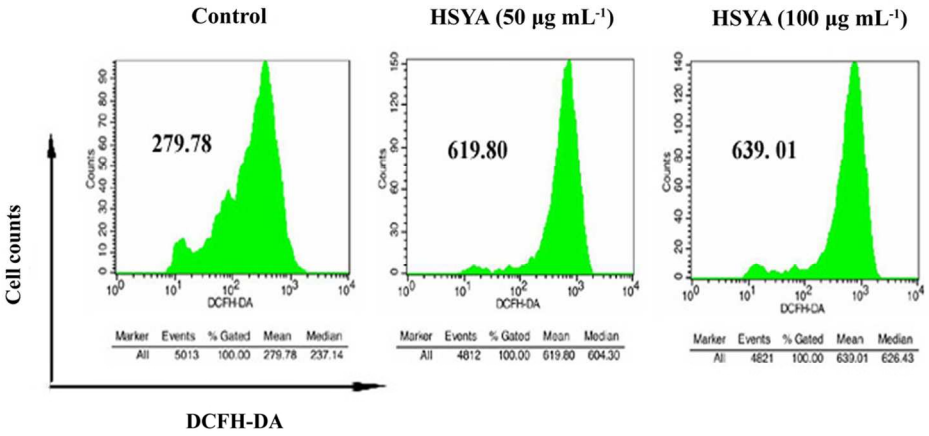

54x32mm (600 x 600 DPI)

Figure 6

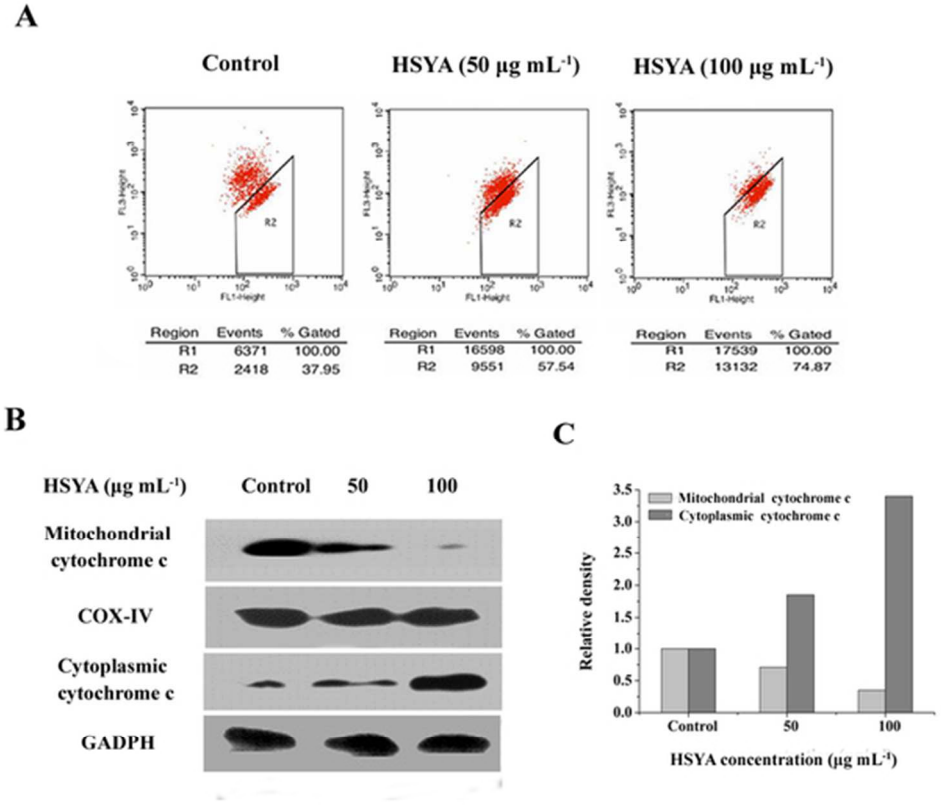

27x24mm (600 x 600 DPI)

Figure 7

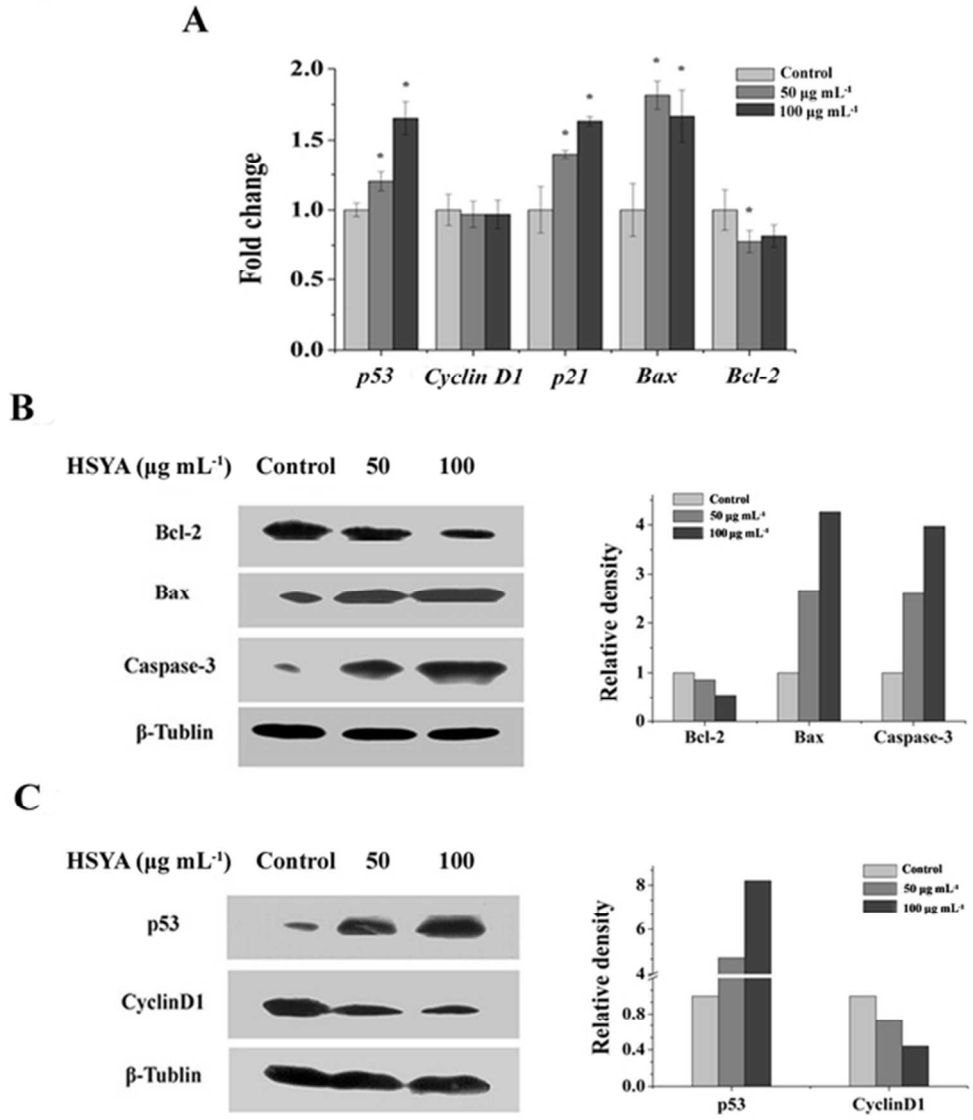

27x32mm (600 x 600 DPI)

Figure 8

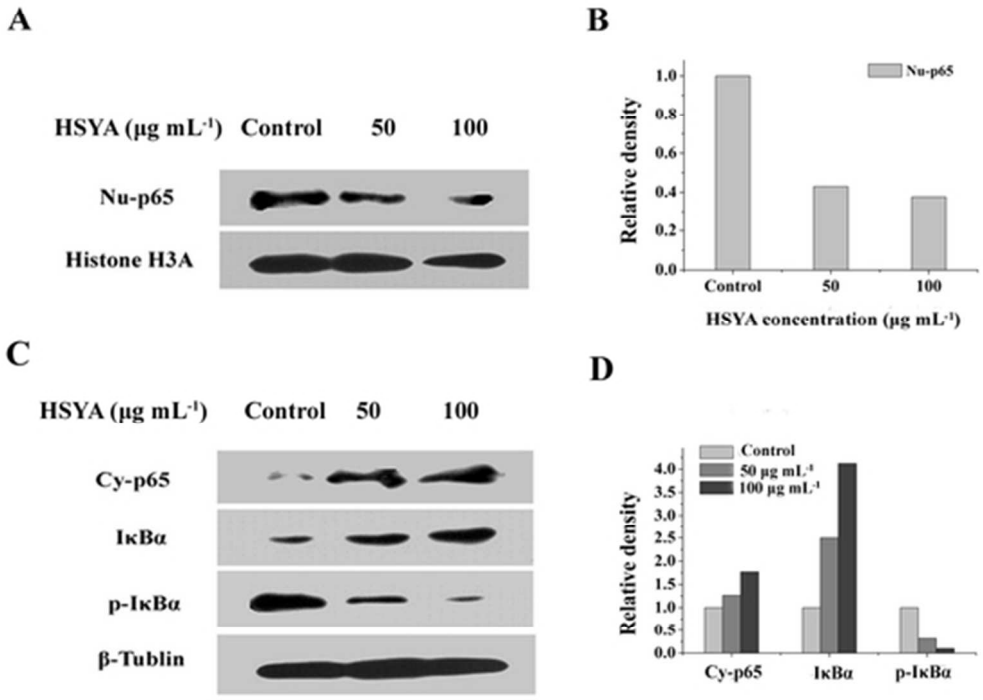

23x19mm (600 x 600 DPI)

Table1 Primers used for Real-time qRT-PCR

Gene	Forward primer (5´-3´)	Reverse primer (5´-3´)
GADPH	CCCATGTTTGTTGTTGGTGTC	TCGTACCATGACTCA AGCTTG
Bcl-2	GGAGGATTGTGGCCTTCTTTGAG	TATGCACCCAGAGTGATGCAGGC
Bax	TGAACTGGACAACATGGAGC	GGTCTTGGATCCAGACAAACAGC
p21	TTGATTAGCAGCGGAACA	TACAGTCTAGGTGGAGAAACG
p53	GCGCACAGAGGA AGA GAA TC	GGCCAACTTGTTCAGTGG AG
CyclinD1	CTGGATGCTGGA GGTCTG CGAGGA	CTGGCATTTTGGAGAGGAAGTGTT